ELSEVIER

NUCLEAR PHYSICS B

High Energy Physics – Theory

Periodic charge oscillations in the Proca theory

Bogdan Damski

Jagiellonian University, Faculty of Physics, Astronomy and Applied Computer Science,
Łojasiewicza 11, 30-348 Kraków, Poland

Abstract

We consider the Proca theory of the real massive vector field. There is a locally conserved 4-current operator in such a theory, which one may use to define the charge operator. Accordingly, there are charged states in which the expectation value of the charge operator is non-zero. We take a close look at the charge operator and study the dynamics of the certain class of charged states. For this purpose, we discuss the mean electric field and 4-current in such states. The mean electric field has the periodically oscillating Coulomb component, whose presence explains the periodic charge oscillations. A complementary insight at such a phenomenon is provided by the mean 4-current, whose discussion leads to the identification of a certain paradox. Last but not least, we show that there is a shock wave propagating in the studied system, which affects analyticity of the mean electric field and 4-current.

1. Introduction

The most economical description of the spin-1 vector field is delivered by the Proca theory, which is defined by the following Lagrangian density [1,2]

$$\mathcal{L} = -\frac{1}{4} F_{\mu\nu} F^{\mu\nu} + \frac{m^2}{2} V_\mu V^\mu, \tag{1}$$

where $F_{\mu\nu} = \partial_\mu V_\nu - \partial_\nu V_\mu$, m is the mass of the vector boson, and V is the vector field operator (we will be referring to the quantum version of the Proca theory unless stated otherwise).

Such an exactly solvable theory–besides delivering insights into physics of both known particles such as ρ and ω mesons and the conjectured ones such a massive photon–provides a fertile playground for the discussion of various issues in quantum field theory. Thus, it should come as no surprise that it appears in such a context in a dozen or so textbooks we are aware of (see e.g. [1,3,4]). This well-documented interest in the Proca theory makes the impression that all of its basic aspects have already been comprehensively discussed. This is why we find it curious that none of the textbooks we have found says anything about the charge operator of the Proca theory and the related issues.

To explain what we are referring to, we write the Proca field equations in the following suggestive form

$$\partial_\mu F^{\mu\nu} = J^\nu, \tag{2}$$

$$J^\nu = -m^2 V^\nu, \tag{3}$$

from which it is immediately seen that the 4-current operator J satisfies the continuity equation

$$\partial \cdot J = 0. \tag{4}$$

This result leads to the following definition of the charge operator

$$Q(t) = \int d^3x \, J^0(t, \boldsymbol{x}) = \int d^3x \, \mathrm{div} \boldsymbol{E}(t, \boldsymbol{x}), \tag{5}$$

where

$$\boldsymbol{E} = \left(F^{i0} \right) \tag{6}$$

is defined in the same way as the electric field operator in the theory of the massless electromagnetic field.

The question now is whether the charge $\langle Q \rangle$, computed as an expectation value of operator (5) in a given state, is conserved in time. This is a non-trivial question because (4) does not guarantee $\partial_t \langle Q \rangle = 0$. It turns out that the situation here is rather unusual because the charge operator in the Proca theory satisfies the harmonic oscillator equation [5,6]. As a result of that, the charge $\langle Q \rangle$ is expected to be time-independent only when it vanishes, which should happen when the mean electric field exhibits faster than inverse-square law asymptotic decay. We are interested in this work in a situation, where the mean electric field asymptotically follows the inverse-square law and the charge periodically oscillates. The main stress in our studies is placed on (i) the construction of charged states in the Proca theory, i.e., the states in which $\langle Q \rangle \neq 0$; (ii) the discussion of the dynamics of the mean electric field and 4-current in such states; and (iii) the discussion of periodic charge oscillations in the Proca theory from the perspective of the special theory of relativity. To the best of our knowledge, none of the (i)–(iii) issues has been addressed in the literature so far (e.g. the harmonic oscillator equation for $Q(t)$ is stated in [5,6] but no discussion touching upon the (i)–(iii) points is provided there).

The outline of this paper is the following. We clarify the charge-related terminology in section 2 and summarize the conventions that we use in appendix A. We gather the fundamental charge operator-related results in section 3, where we also provide some comments placing our research in a larger context. We introduce and formally characterize a certain class of charged states in section 4, the simplest one illustrating the periodic charge oscillations. We present

the thorough discussion of the dynamics of one such state in section 5.[1] These considerations are then generalized in section 6, where we comment on the dynamics of the whole family of charged states. The numerous technical details, pertinent to the discussion in section 5 (section 6), are comprehensively laid out in appendices B and C (appendices D and E). The conceptual relativity-related issues associated with periodic charge oscillations are discussed in section 7. The summary of our work is provided in section 8.

2. Terminology

To begin, we consider the classical theory for a moment and mention that the timelike component of a locally conserved 4-current is traditionally called a charge density in various physical systems. As a result of that, $J^0 = \mathrm{div}\boldsymbol{E} = -m^2 V^0$ could be termed in such a way as well. A bit different terminology was proposed in [2], where the Proca theory in the presence of "ordinary" charged particles was considered. Then $\mathrm{div}\boldsymbol{E} = -m^2 V^0 + \rho$ with ρ representing the charge density of such particles. In this context, $-m^2 V^0$ was termed as a pseudocharge density.

We shall not dwell on which one of these two names is more appropriate. Coming back to the quantum theory, we conclude that $J^0 = -m^2 V^0$ will be called the charge density operator. In accord with that, $\boldsymbol{J} = -m^2 \boldsymbol{V}$ will be called the charge current operator, where we have simplified the terminology by skipping the term "density" (the same simplification has been applied in section 1 to the name of the operator J). $\boldsymbol{E}$ and $\boldsymbol{B} = \mathrm{rot}\boldsymbol{V}$ will be called the electric and magnetic field operators, without stressing the fact that they are defined in the massive theory. Finally, for the sake of brevity, the expectation value of the operators $\boldsymbol{E}$, $\boldsymbol{J}$, etc. will be called the mean electric field, the mean 4-current, etc.

3. Charge operator

We discuss here some elementary observations about the charge operator, setting the stage for the presentation of our key findings in the subsequent sections.

To begin, we provide the expression for the vector field operator V [1]

$$V^\mu(x) = \int \frac{d^3k}{(2\pi)^{3/2}} \frac{1}{\sqrt{2\varepsilon_k}} \sum_{\sigma=1}^{3} \epsilon^\mu(\boldsymbol{k}, \sigma)[a_{\boldsymbol{k}\sigma} \exp(-\mathrm{i}k \cdot x) + \mathrm{h.c.}], \tag{7a}$$

where $k^0 = \varepsilon_k = \sqrt{m^2 + \omega_k^2}$, $\omega_k = |\boldsymbol{k}|$,

$$[a_{\boldsymbol{k}\sigma}, a_{\boldsymbol{k}'\sigma'}] = 0, \;\; [a_{\boldsymbol{k}\sigma}, a_{\boldsymbol{k}'\sigma'}^\dagger] = \delta_{\sigma\sigma'}\delta(\boldsymbol{k} - \boldsymbol{k}') \tag{7b}$$

for $\sigma, \sigma' = 1, 2, 3$,

$$\epsilon(\boldsymbol{k}, \ell) = (0, \boldsymbol{\epsilon}(\boldsymbol{k}, \ell)), \tag{7c}$$

$$\boldsymbol{\epsilon}(\boldsymbol{k}, \ell) \cdot \boldsymbol{k} = 0, \;\; \boldsymbol{\epsilon}(\boldsymbol{k}, \ell) \cdot \boldsymbol{\epsilon}(\boldsymbol{k}, \ell') = \delta_{\ell\ell'} \tag{7d}$$

for $\ell, \ell' = 1, 2$, and

---

[1] While talking about the dynamics of charged states, we tacitly refer to the Schrödinger picture formulation of the problem, which is convenient on different occasions. However, our calculations involving field operators have been done in the Heisenberg picture, and so they are presented in such a standard "language".

$$\epsilon(\boldsymbol{k}, 3) = \left(\frac{\omega_k}{m}, \frac{\varepsilon_k}{m} \hat{\boldsymbol{k}} \right), \quad \hat{\boldsymbol{k}} = \boldsymbol{k}/\omega_k. \tag{7e}$$

We mention in passing that the transverse polarization vectors are assumed to be real and satisfy

$$\sum_{\ell=1}^{2} \epsilon^i(\boldsymbol{k}, \ell) \epsilon^j(\boldsymbol{k}, \ell) = \delta_{ij} - k^i k^j / \omega_k^2. \tag{8}$$

Two operators can be now discussed: the 4-current operator J (3) and the electric field operator $\boldsymbol{E}$ [1]

$$\boldsymbol{E}(x) = \mathrm{i}m \int \frac{d^3k}{(2\pi)^{3/2}} \frac{\hat{\boldsymbol{k}}}{\sqrt{2\varepsilon_k}} [a_{\boldsymbol{k}3} \exp(-\mathrm{i}k \cdot x) - \mathrm{h.c.}]$$

$$+ \mathrm{i} \int \frac{d^3k}{(2\pi)^{3/2}} \sqrt{\frac{\varepsilon_k}{2}} \sum_{\sigma=1}^{2} \epsilon(\boldsymbol{k}, \sigma) [a_{\boldsymbol{k}\sigma} \exp(-\mathrm{i}k \cdot x) - \mathrm{h.c.}], \tag{9}$$

where again $k^0 = \varepsilon_k$. These operators are interlinked via $J^0 = \mathrm{div}\, \boldsymbol{E}$. Somewhat more interestingly, J and $\boldsymbol{E}$ are also interconnected via

$$[E^i(t, \boldsymbol{x}), J^s(t, \boldsymbol{y})] = -\mathrm{i}m^2 \delta_{is} \delta(\boldsymbol{x} - \boldsymbol{y}), \tag{10}$$

which follows from the canonical commutation relations (E_i are the canonical conjugates of the fields V^i). Moreover, it is implied by (10) that

$$[J^0(t, \boldsymbol{x}), J^s(t, \boldsymbol{y})] = -\mathrm{i}m^2 \frac{\partial}{\partial x^s} \delta(\boldsymbol{x} - \boldsymbol{y}). \tag{11}$$

Next, we turn our attention to the charge operator, which is obtained by combining (3), (5), and (7). The resulting expression, however, has to be treated with some care. We proceed by considering the following regularized expression for the charge operator

$$\int d^3x \exp(-\epsilon |\boldsymbol{x}|^2) J^0(t, \boldsymbol{x}) = -m(2\pi)^{3/2} \int d^3k \frac{\omega_k \delta_\epsilon(\boldsymbol{k})}{\sqrt{2\varepsilon_k}} [a_{\boldsymbol{k}3} \exp(-\mathrm{i}\varepsilon_k t) + \mathrm{h.c.}], \tag{12a}$$

where $\epsilon > 0$ and

$$\delta_\epsilon(\boldsymbol{k}) = \frac{1}{(2\sqrt{\pi \epsilon})^3} \exp\left(-\frac{\omega_k^2}{4\epsilon} \right) \tag{12b}$$

is the nascent delta function. The above ϵ-regularization controls the size of the spatial integration region, which is useful during the exchange of the order of spatial (d^3x) and momentum (d^3k) integrations in (12). The thermodynamic limit expression for the charge operator is recovered by taking ϵ to 0^+, which brings us to

$$Q(t) = \lim_{\epsilon \to 0^+} Q_\epsilon(t), \tag{13a}$$

$$Q_\epsilon(t) = -\sqrt{\frac{m}{2}} (2\pi)^{3/2} \int d^3k \, \omega_k \delta_\epsilon(\boldsymbol{k}) [a_{\boldsymbol{k}3} \exp(-\mathrm{i}mt) + \mathrm{h.c.}]. \tag{13b}$$

Explicit time dependence of the charge operator, which happens despite the fact that the 4-current operator satisfies continuity equation (4), provokes the question of what differential equation governs the evolution of $Q(t)$. It turns out that the charge operator satisfies the harmonic oscillator equation

$$\ddot{Q}(t) = -m^2 Q(t), \tag{14}$$

where each dot stands for d/dt. Such a result instantly follows from the differentiation of (13). Alternatively, one may obtain it by means of the Heisenberg equation

$$\ddot{Q}(t) = \lim_{\epsilon \to 0^+} [H, [Q_\epsilon(t), H]], \tag{15a}$$

$$H = \int d^3k \, \varepsilon_k \sum_{\sigma=1}^{3} a_{k\sigma}^\dagger a_{k\sigma}, \tag{15b}$$

where H is the Hamiltonian of the Proca theory. Having said all that, we would like to discuss the general context of results (10)–(14).

First, (10) and (11) can be compared to the Schwinger's prediction about the structure of electric field–current and charge density–current commutators [7]. Namely, based on general considerations, Schwinger proposed that

$$\langle [E^i(t, \boldsymbol{x}), j^s(t, \boldsymbol{y})] \rangle = -\mathrm{i} K^2 \delta_{is} \delta(\boldsymbol{x} - \boldsymbol{y}), \tag{16}$$

$$\langle [j^0(t, \boldsymbol{x}), j^s(t, \boldsymbol{y})] \rangle = -\mathrm{i} K^2 \frac{\partial}{\partial x^s} \delta(\boldsymbol{x} - \boldsymbol{y}), \tag{17}$$

where the expectation values are computed in the vacuum state, K is a constant that could be formally infinite, and j is the 4-current operator in the system with the charge-bearing matter field (the Dirac field or the complex Klein-Gordon field coupled to the electromagnetic field). Note that (10) and (11), obtained in the theory decoupled from any matter field, have exactly the same structure as (16) and (17) with $K = m$.

Second, (12)–(14) can be discussed in the context of the symmetry breaking studies comprehensively reviewed in [6]. To begin, the procedure of the evaluation of charge operators in the restricted area of space is discussed in [6]. Its particular realization is seen in (12). Next, we note that the charge operator of the Proca theory has a singular infrared structure, just as charge operators studied in [6].[2] As it does not lead to any problems in our work, we will not dwell on it. Finally, the harmonic oscillator equation for the charge operator of the massive vector field appeared in seminal paper [5] and review [6]. In these references, however, such an equation is merely stated. Given the popularity of [5], we find it curious that, to the best of our knowledge, the harmonic dynamics of the charge in the Proca theory has not really been discussed in the literature so far (see also the last paragraph of this section for further discussion of this observation).

Till the end of this section, we provide simple remarks pertaining to the harmonic oscillator equation satisfied by the charge operator. The general solution of (14) reads

$$Q(t) = Q(0) \cos(mt) + \frac{\dot{Q}(0)}{m} \sin(mt), \tag{18}$$

from which the periodic charge conservation law is instantly obtained. Defining

$$\mathcal{Q}(t) = \langle Q(t) \rangle, \quad \dot{\mathcal{Q}}(t) = \langle \dot{Q}(t) \rangle, \tag{19}$$

---

[2] To illustrate the singular character of (13), we remark that when one tries to compute the norm of the state $Q(t)|0\rangle$, one obtains the poorly-defined expression involving the product of two nascent delta functions having the same momentum argument. We note that the problems with the computation of such a norm are expected on general grounds (see [8] as well as the comments about this paper below equation (2.5) of [6]).

where the expectation value is taken in a normalizable time-independent Heisenberg-picture state, we get

$$\mathcal{Q}(t) = \mathcal{Q}(0)\cos(mt) + \frac{\dot{\mathcal{Q}}(0)}{m}\sin(mt). \tag{20}$$

The usual charge conservation law, $\dot{\mathcal{Q}}(t) = 0$, is only seen when

$$\mathcal{Q}(0) = \dot{\mathcal{Q}}(0) = 0. \tag{21}$$

For example, this is the case in any state of the form

$$c|0\rangle + \int d^3k \sum_{\sigma=1}^{2} c_\sigma(\boldsymbol{k}) a_{\boldsymbol{k}\sigma}^\dagger |0\rangle + \int d^3k\, d^3k' \sum_{\sigma,\sigma'=1}^{2} c_{\sigma\sigma'}(\boldsymbol{k}, \boldsymbol{k}') a_{\boldsymbol{k}\sigma}^\dagger a_{\boldsymbol{k}'\sigma'}^\dagger |0\rangle + \cdots \tag{22}$$

or

$$\int d^3k \sum_{\sigma=1}^{3} c_\sigma(\boldsymbol{k}) a_{\boldsymbol{k}\sigma}^\dagger |0\rangle, \tag{23}$$

where $|0\rangle$ is the vacuum state of the Proca theory and the complex-valued c, $c_\sigma(\boldsymbol{k})$, $c_{\sigma\sigma'}(\boldsymbol{k}, \boldsymbol{k}')$, etc. are constrained so as to make the above states normalizable.

A markedly different situation takes place when (21) is not satisfied. The total charge is only periodically conserved then. Its oscillation period,

$$\frac{2\pi}{m}, \tag{24}$$

depends on the mass of the vector boson described by the Proca theory. We note that a similar scenario was mentioned in [9] in the context of spatially unbounded superconductors. In these non-relativistic mean-field considerations, the role of the mass m is played by the plasma frequency(ies).

We are interested in this work in finding the detailed explanation of the periodic charge oscillations in the Proca theory. For that purpose, we will analyze the dynamics of the states in which the long-distance decay of the mean electric field follows the inverse-square law. To the best of our knowledge, such studies have not been reported before. This observation may be explained by the fact that the short-range electric field is traditionally discussed in the context of the massive photon theories. It is presumably so because localized external sources are expected in such theories to create the exponentially decaying electric field (the total charge for such a field vanishes and as such it is conserved; see [10] for a concrete example where not only the total charge but also the one enclosed in a finite volume is discussed in the presence of the short-range electric field). However, it should be stressed that finite-energy normalizable states, in which the mean electric field asymptotically satisfies the inverse-square law, *do* exist in the Hilbert space of the Proca theory. As the periodic charge conservation law implies, they cannot be stationary. The theoretical characterization of their non-trivial dynamics is the main goal of this work.

4. Charged states

Charged states in the Proca theory can be constructed in an innumerable number of ways. The simplest of them are built of the vacuum state and the Fock states containing just one longitudinal field excitation. The particular class of such states will be commented upon below.

To proceed, we introduce

$$\chi(\boldsymbol{x}) = \frac{ie}{m} \int \frac{d^3k}{(2\pi)^{3/2}} f(\omega_k) \sqrt{\frac{\varepsilon_k}{2\omega_k^2}} [a_{\boldsymbol{k}3} \exp(i\boldsymbol{k} \cdot \boldsymbol{x}) - \text{h.c.}], \qquad (25)$$

where e is the electric charge unit and f is a dimensionless real function. The form of χ is chosen such that

$$\left[\int d^3y \, \exp\left(-\epsilon|\boldsymbol{y}|^2\right) J^0(t, \boldsymbol{y}), \chi(\boldsymbol{x}) \right] = ie \int d^3k \, f(\omega_k)\delta_\epsilon(\boldsymbol{k}) \cos(\varepsilon_k t + \boldsymbol{k} \cdot \boldsymbol{x}), \qquad (26)$$

which guarantees

$$[Q(t), \chi(\boldsymbol{x})] = ief(0) \cos(mt). \qquad (27)$$

This suggests consideration of the state

$$|\psi(\boldsymbol{x})\rangle = [\alpha - i\beta\chi(\boldsymbol{x})] |0\rangle, \qquad (28)$$

where the dimensionless real parameters α, β are non-zero. Two remarks are in order now.

First, we require that $\langle\psi|\psi\rangle = 1$, which leads to

$$1 = \alpha^2 + \beta^2 \frac{e^2}{4\pi^2 m^2} \int\limits_0^\infty d\omega_k f^2(\omega_k)\varepsilon_k. \qquad (29)$$

Such a relation is meaningful as long as the above integral is convergent. This will be guaranteed by asking that the mean energy is finite

$$\mathcal{H} = \langle\psi(\boldsymbol{x})|H|\psi(\boldsymbol{x})\rangle = \beta^2 \frac{e^2}{4\pi^2 m^2} \int\limits_0^\infty d\omega_k f^2(\omega_k)\varepsilon_k^2 < \infty. \qquad (30)$$

Second, the mean charge stored in state (28) can be easily computed by means of (27)

$$\mathcal{Q}(t) = \langle\psi(\boldsymbol{x})|Q(t)|\psi(\boldsymbol{x})\rangle = \alpha\beta f(0)e \cos(mt). \qquad (31)$$

This expression underscores the role of the infrared sector in the discussed problem and it tells us that $0 < |f(0)| < \infty$ is of interest in the context of periodic charge oscillations. We employ the following "normalization" of the function f

$$f(0) = 1. \qquad (32)$$

Upon such a choice, the amplitude of periodic charge oscillations reads

$$q = \alpha\beta e. \qquad (33)$$

Further insights into the periodic charge oscillations can be obtained from two interrelated quantities: the mean electric field and 4-current.

The mean electric field–obtained by combining (9), (25), (28), and (33)–reads

$$\mathcal{E}(t, \boldsymbol{r}) = \langle\psi(\boldsymbol{x})|\boldsymbol{E}(t, \boldsymbol{y})|\psi(\boldsymbol{x})\rangle = -\frac{q\hat{\boldsymbol{r}}}{2\pi^2} \int\limits_0^\infty d\omega_k f(\omega_k)\partial_r \frac{\sin(\omega_k r)}{\omega_k r} \cos(\varepsilon_k t), \qquad (34)$$

where $\hat{\boldsymbol{r}} = \boldsymbol{r}/|\boldsymbol{r}|$, $r = |\boldsymbol{r}|$, and $\boldsymbol{r} = \boldsymbol{y} - \boldsymbol{x}$. This expression, under the assumption that the derivative can be taken outside the integral,[3] can be cast into the following suggestive form

$$\mathcal{E}(t, \boldsymbol{r}) = -\nabla\phi(t, r), \tag{35a}$$

$$\phi(t, r) = \frac{q}{2\pi^2 r} \int\limits_0^\infty d\omega_k \, f(\omega_k) \frac{\sin(\omega_k r)}{\omega_k} \cos(\varepsilon_k t). \tag{35b}$$

The mean 4-current reads

$$\mathcal{J}^0(t, r) = \langle\psi(\boldsymbol{x})| - m^2 V^0(t, \boldsymbol{y})|\psi(\boldsymbol{x})\rangle = \mathrm{div}\mathcal{E}(t, \boldsymbol{r}), \tag{36}$$

$$\boldsymbol{\mathcal{J}}(t, r) = \langle\psi(\boldsymbol{x})| - m^2 V(t, \boldsymbol{y})|\psi(\boldsymbol{x})\rangle = -\partial_t \mathcal{E}(t, \boldsymbol{r}), \tag{37}$$

where one has to be aware that an ambiguity may arise during the evaluation of (36) and (37); see section 5.1 for details.

Non-trivial dynamics captured by (35)–(37) will be comprehensively analyzed in a specific case in the next section. Before jumping right there, however, we would like to briefly comment on the following issues.

First, ϕ plays the role of the electric field potential in (35). Second, the last equality in (36) originates from $J^0 = \mathrm{div}\boldsymbol{E}$. Third, the last equality in (37) can be explained by combining the Proca equation $\mathrm{rot}\boldsymbol{B} = \boldsymbol{J} + \partial_t \boldsymbol{E}$ with the observation that the mean magnetic field trivially vanishes in the studied states because no transverse modes are populated in them.

5. Example of periodic charge oscillations

We illustrate here the concepts introduced in section 4. For this purpose, we consider

$$f(\omega_k) = \left(\frac{m}{\varepsilon_k}\right)^2, \tag{38}$$

which leads to an elegant analytical solution.

To begin, we mention that the evaluation of (29) and (30) yields

$$1 = \alpha^2 + \beta^2 \frac{e^2}{4\pi^2}, \tag{39}$$

$$\mathcal{H} = \beta^2 m \frac{e^2}{8\pi}. \tag{40}$$

The integrals leading to such results are straightforwardly computed with the help of mapping (B.2a) and the following formula

$$\int\limits_0^\infty \frac{dx}{\mathrm{ch}^b(x)} = \frac{\sqrt{\pi}}{2} \frac{\Gamma(b/2)}{\Gamma(b/2 + 1/2)} \quad \text{for } b > 0, \tag{41}$$

which can be obtained from expression 3.518.3 listed in [11].

---

[3] Such an operation, in the expression for the mean electric field, can be performed without any complications in specific yet fairly representative problems discussed in sections 5 and 6. We shall not dwell on the general conditions allowing for it.

Combining (39) with (33), we find that

$$\alpha = \frac{\exp(i\sigma)}{\sqrt{2}} \sqrt{1 \pm \sqrt{1 - \frac{q^2}{\pi^2}}}, \tag{42}$$

$$\beta = \sqrt{2}\frac{\pi}{e} \sqrt{1 \mp \sqrt{1 - \frac{q^2}{\pi^2}}}, \tag{43}$$

where σ is equal to 0 (π) for q greater (smaller) than zero. These expressions show that the amplitude of periodic charge oscillations in the studied problem is upper bounded by π. There is nothing fundamental about such an elegant bound because it depends on the particular form of the function f (section 6).

Next, we note that the electric field potential in the studied problem reads

$$\phi(t,r) = \frac{q}{2\pi^2 r} \int\limits_0^\infty d\omega_k \left(\frac{m}{\varepsilon_k}\right)^2 \frac{\sin(\omega_k r)}{\omega_k} \cos(\varepsilon_k t). \tag{44}$$

The hint of what we are dealing here with comes from

$$\phi(0,r) = q\frac{1 - \exp(-mr)}{4\pi r}, \tag{45}$$

which has been obtained from (B.22). This result implies that initially, i.e. at $t = 0$, there is the Coulomb field in our system from which the Debye field is subtracted. The former field certainly needs no introduction, the latter typically appears in the studies of plasmas and electrolytes, where it captures the screening of the Coulomb field of the test charge inside such systems. Equation (45) triggers two remarks.

Technically, the above-mentioned subtraction makes the energy finite and it can be seen as one of the many examples of how the Coulomb field may be regularized at short distances. Note that while other regularizations can be introduced by changing the function f, the Coulomb component of (45) is fixed by the requirement that $\mathcal{Q}(0) = q$ [see (56)].

Physically, neither the Coulomb nor Debye field is external source-generated in the studied problem. This implies that the mean electric field will necessarily evolve in time.

Having discussed the situation at $t = 0$, we are ready to study the dynamics for $t > 0$. The evaluation of the integral from (44) is presented in appendix B. It leads to the following result. For $r \geq t > 0$

$$\phi(t,r) = q\frac{\cos(mt) - \exp(-mr)}{4\pi r}, \tag{46}$$

whereas for $0 < r < t$

$$\phi(t,r) = q\frac{\cos(mr) - \exp(-mr)}{4\pi r} - \frac{q}{4\pi r} \int\limits_{mr}^{mt} dy \int\limits_0^{mr} dx \mathrm{J}_0\left(\sqrt{y^2 - x^2}\right), \tag{47}$$

where J_n is the Bessel function of the first kind of order n (it should not be confused with the n-th covariant component of the 4-current operator J). The following conclusions come from the analysis of these expressions.

5.1. Shock wave front

The curious division of space into the $r \geq t$ and $0 < r < t$ regions, exhibited by (46) and (47), comes from the fact that $\phi(t, r)$ is singular on the sphere $r = t$. It turns out that there is a shock wave in $\phi(t, r)$ propagating outwards from the point $\boldsymbol{r} = \boldsymbol{0}$ with the speed of light. Namely, while $\phi(t, r)$, $\partial_r \phi(t, r)$, and $\partial_t \phi(t, r)$ are continuous across $r = t$, the second order derivatives of $\phi(t, r)$ are discontinuous there. The subtle issues associated with the differentiation of $\phi(t, r)$ are also seen from the fact that while

$$\partial_\xi \int_0^\infty d\omega_k \left(\frac{m}{\varepsilon_k}\right)^2 \frac{\sin(\omega_k r)}{\omega_k} \cos(\varepsilon_k t) = \int_0^\infty d\omega_k \left(\frac{m}{\varepsilon_k}\right)^2 \partial_\xi \left(\frac{\sin(\omega_k r)}{\omega_k} \cos(\varepsilon_k t)\right) \tag{48}$$

holds for any $r, t > 0$,

$$\partial_\eta \partial_\xi \int_0^\infty d\omega_k \left(\frac{m}{\varepsilon_k}\right)^2 \frac{\sin(\omega_k r)}{\omega_k} \cos(\varepsilon_k t) = \int_0^\infty d\omega_k \left(\frac{m}{\varepsilon_k}\right)^2 \partial_\eta \partial_\xi \left(\frac{\sin(\omega_k r)}{\omega_k} \cos(\varepsilon_k t)\right) \tag{49}$$

holds for $r, t > 0$ except $r = t$ (ξ represents either t or r and so does η). These observations come from the results presented in appendices B.4 and C. The following remarks are in order now.

First, (48) guarantees that $\langle \psi | \boldsymbol{E} | \psi \rangle = -\boldsymbol{\nabla} \phi$ for all $r, t > 0$. Such a mean electric field–with the help of (46), (47), and the results presented in appendix C.1–can be written in the following suggestive form

$$\boldsymbol{\mathcal{E}}(t, \boldsymbol{r}) = \hat{\boldsymbol{r}} \mathcal{A}(t, r) + \frac{qm^2 \hat{\boldsymbol{r}}}{8\pi t} |t - r| + O\left((t - r)^2\right), \tag{50}$$

where $\mathcal{A}(t, r)$, $\partial_t \mathcal{A}(t, r)$, and $\partial_r \mathcal{A}(t, r)$ are continuous in the neighborhood of $r = t$.

Second, we turn our attention to the mean 4-current. The equality in (49) for $r \neq t$ means that for such r, t we have $\mathcal{J}^0 = \langle \psi | -m^2 V^0 | \psi \rangle = \text{div}\boldsymbol{\mathcal{E}}$ and $\boldsymbol{\mathcal{J}} = \langle \psi | -m^2 \boldsymbol{V} | \psi \rangle = -\partial_t \boldsymbol{\mathcal{E}}$. A quick look at (50) reveals that these two quantities must be discontinuous across $r = t$. Such a propagating discontinuity, i.e. a shock wave, is illustrated by the following formulas

$$\frac{qm^2}{4\pi t} = \lim_{r \to t^+} \mathcal{J}^0(t, r) - \lim_{r \to t^-} \mathcal{J}^0(t, r), \tag{51}$$

$$\frac{qm^2 \hat{\boldsymbol{r}}}{4\pi t} = \lim_{r \to t^+} \boldsymbol{\mathcal{J}}(t, r\hat{\boldsymbol{r}}) - \lim_{r \to t^-} \boldsymbol{\mathcal{J}}(t, r\hat{\boldsymbol{r}}), \tag{52}$$

which can be derived from (50).

Third, exactly at the $r = t$ shock wave front, we find with the help of the results presented in appendix C.2 that $\langle \psi | -m^2 V^0 | \psi \rangle$ and $\langle \psi | -m^2 \boldsymbol{V} | \psi \rangle$ are given by

$$qm^2 \frac{\exp(-mt) - 1/2}{4\pi t}, \; qm\hat{\boldsymbol{r}} \frac{\sin(mt) - mt/2}{4\pi t^2}. \tag{53}$$

At the same time, however,

$$\text{div}\boldsymbol{\mathcal{E}} = \text{undefined}, \; -\partial_t \boldsymbol{\mathcal{E}} = \text{undefined} \tag{54}$$

at $r = t$, which is seen from (50). These results lead to the following observations.

To begin, we note that the discrepancy between (53) and (54) implies that the last equalities in (36) and (37) do not hold at $r = t$ when $f(\omega_k)$ is given by (38). This is caused by the fact that (49) does not hold at $r = t$.

Then, we remark that the difference between (53) and (54) raises the question of whether $\mathcal{J}^0(t, t)$ and $\boldsymbol{\mathcal{J}}(t, t\hat{\boldsymbol{r}})$ can be unambiguously computed. As we are unsure how to convincingly address this issue, we shall leave open the question of what is the value of $\mathcal{J}^0(t, t)$ and $\boldsymbol{\mathcal{J}}(t, t\hat{\boldsymbol{r}})$ in the considered problem. We only mention that the discussed ambiguity is not generic in the sense that it can be removed by increasing the decay rate of $f(\omega_k \to \infty)$. This is illustrated in section 6, where $\mathcal{J}^0(t, t)$ and $\boldsymbol{\mathcal{J}}(t, t\hat{\boldsymbol{r}})$ are straightforwardly computed.

All in all, we find it remarkable that there is a genuine shock wave discontinuity in the studied problem despite the fact that the energy associated with the analyzed solution is finite (40).

5.2. From shock wave front to spatial infinity

We are interested here in the region of space $r > t$, where (46) holds. The mean electric field obtained from such an expression reads

$$\boldsymbol{\mathcal{E}}(t, \boldsymbol{r}) = \frac{q\hat{\boldsymbol{r}}}{4\pi r^2} \cos(mt) - \frac{q\hat{\boldsymbol{r}} \exp(-mr)}{4\pi r^2}(1 + mr). \tag{55}$$

Several remarks are in order now.

First of all, the first term in (55) represents the *periodically oscillating* Coulomb field. Such a field, to the best of our knowledge, has not been previously discussed in the literature. The second term in (55) is the Debye field, which is frozen in its $t = 0$ arrangement (see section 6 for the dynamical but aperiodic version of such a field).

Second, the Debye component of (55) is short-range and so it does not affect the periodic charge oscillations. Their amplitude and period can be instantly read from the Coulomb component of (55) because

$$\mathcal{Q}(t) = \lim_{r \to \infty} \int d\boldsymbol{S}(\boldsymbol{r}) \cdot \boldsymbol{\mathcal{E}}(t, \boldsymbol{r}) = q \cos(mt), \tag{56}$$

where $d\boldsymbol{S}$ is the surface element. It should be now stressed that such a result has been obtained without the use of any regularization. Therefore, it supports the ϵ-regularization procedure discussed in section 3 because the very same result is also obtained by computing the expectation value of (13).

Third, the charge stored in the $r > t$ region of space is

$$\mathcal{Q}(t, r > t) = \int\limits_{r > t} d^3r \, \mathcal{J}^0(t, r) = q \exp(-mt)(1 + mt). \tag{57}$$

It becomes exponentially small for $mt \gg 1$.

Fourth, the mean 4-current reads

$$\mathcal{J}^0(t, r) = \frac{qm^2}{4\pi r} \exp(-mr), \tag{58}$$

$$\boldsymbol{\mathcal{J}}(t, \boldsymbol{r}) = \frac{qm\hat{\boldsymbol{r}}}{4\pi r^2} \sin(mt). \tag{59}$$

A trivial calculation confirms that $\partial \cdot \mathcal{J} = 0$.

5.3. Behind shock wave front

The $0 < r < t$ region of space is of interest here, where the mean electric field and 4-current are given by the following formulas
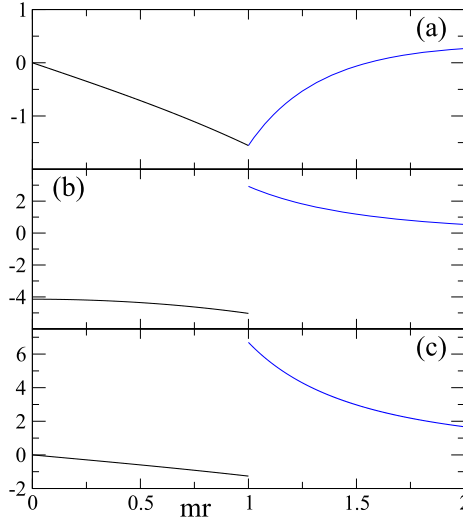
Fig. 1. The mean values of various quantities characterizing the properties of the system at $mt = 1$. Panel (a): the rescaled radial component of the electric field, $\mathcal{E} \cdot \hat{\boldsymbol{r}} \times 10^2 q^{-1} m^{-2}$ obtained from (55) and (60). Panel (b): the rescaled charge density, $\mathcal{J}^0 \times 10^2 q^{-1} m^{-3}$ obtained from (58) and (61). Panel (c): the rescaled radial component of the charge current, $\mathcal{J} \cdot \hat{\boldsymbol{r}} \times 10^2 q^{-1} m^{-3}$ obtained from (59) and (62). The black and blue lines show $r < t$ and $r > t$ results, respectively.

$$\mathcal{E}(t, \boldsymbol{r}) = \frac{\hat{\boldsymbol{r}} \phi(t, r)}{r} - \frac{q m \hat{\boldsymbol{r}} \exp(-mr)}{4\pi r} + \frac{q m \hat{\boldsymbol{r}}}{4\pi r} \int\limits_{mr}^{mt} dx \mathrm{J}_0\left(\sqrt{x^2 - (mr)^2}\right), \tag{60}$$

$$\mathcal{J}^0(t, r) = \frac{q m^2}{4\pi r} \exp(-mr) - \frac{q m^2}{4\pi r} + \frac{q m^3}{4\pi} \int\limits_{mr}^{mt} dx \frac{\mathrm{J}_1\left(\sqrt{x^2 - (mr)^2}\right)}{\sqrt{x^2 - (mr)^2}}, \tag{61}$$

$$\mathcal{J}(t, \boldsymbol{r}) = \frac{q m \hat{\boldsymbol{r}}}{4\pi r^2} \int\limits_{0}^{mr} dx \mathrm{J}_0\left(\sqrt{(mt)^2 - x^2}\right) - \frac{q m^2 \hat{\boldsymbol{r}}}{4\pi r} \mathrm{J}_0\left(m\sqrt{t^2 - r^2}\right). \tag{62}$$

Several remarks are in order now.

First, these results are obtained from electric field potential (47), which explicitly appears in (60). As can be checked, (61) and (62) satisfy $\partial \cdot \mathcal{J} = 0$.

Second, as the above quantities are given by fairly complicated expressions, we plot them on Figs. 1–4 (note that the rescaling factors used in Fig. 1 are two orders of magnitude smaller than the ones employed in Figs. 2–4). Fig. 1 provides the representative illustration of (60)–(62) in the short-time limit. Figs. 2–4 representatively display what happens in the long-time limit. Namely, the shock wave front leaves behind spatial oscillations of $\mathcal{E}$, $\mathcal{J}^0$, and $\mathcal{J}$. As can be numerically verified, the number of such oscillations increases as the time goes by while their amplitude decreases.

Third, the above-mentioned oscillations are quite dramatic. Indeed, for large-enough times the mean electric field and charge current reverse their direction several times in the studied region of space. Similarly, the charge density changes its sign several times there. Clearly, a curious dynamics is seen in Figs. 2–4, strikingly different from the one discussed in section 5.2.
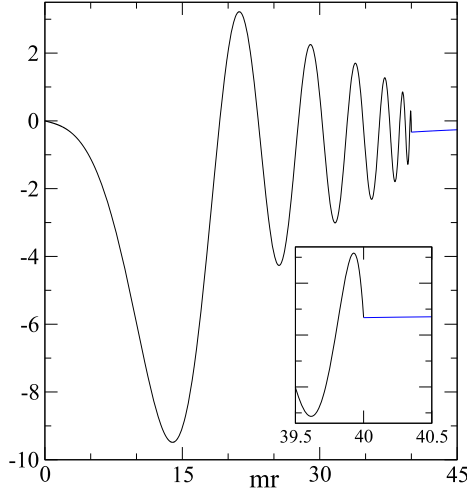
Fig. 2. The rescaled radial component of the mean electric field. Namely, $\mathcal{E} \cdot \hat{r} \times 10^4 q^{-1} m^{-2}$ at $mt = 40$. The black line comes from (60), whereas the blue one is obtained from (55). The inset magnifies the area around the shock wave front, where the slope of the plotted quantity discontinuously changes.
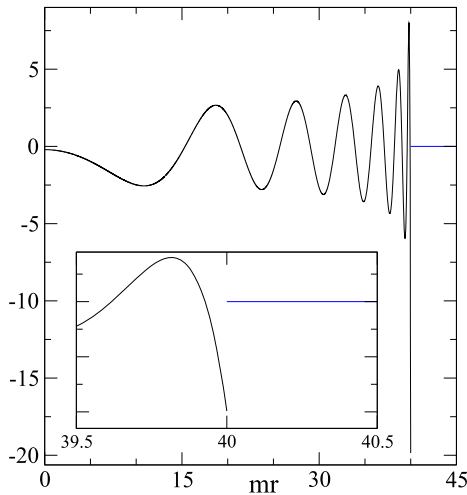

Fig. 3. The rescaled mean charge density. Namely, $\mathcal{J}^0 \times 10^4 q^{-1} m^{-3}$ at $mt = 40$. The black line comes from (61), whereas the blue one is obtained from (58). The inset magnifies the shock wave discontinuity.

Formulas (60)–(62) can be simplified near $r = 0$ and $r = t^-$. In the latter case

$$\lim_{r \to t^-} \mathcal{E}(t, r\hat{r}) = q\hat{r} \frac{\cos(mt) - (1 + mt) \exp(-mt)}{4\pi t^2}, \tag{63}$$

$$\lim_{r \to t^-} \mathcal{J}^0(t, r) = qm^2 \frac{\exp(-mt) - 1}{4\pi t}, \tag{64}$$

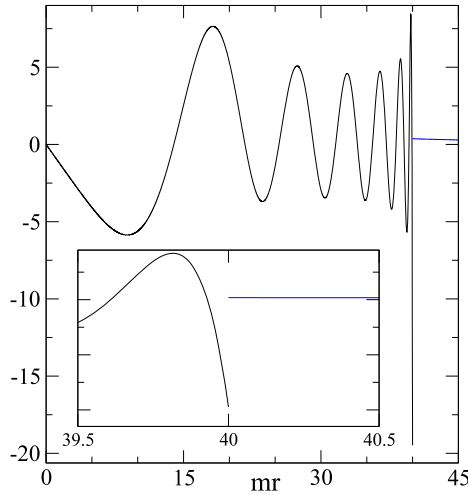$$\lim_{r \to t^-} \mathcal{J}(t, r\hat{r}) = qm\hat{r} \frac{\sin(mt) - mt}{4\pi t^2}. \tag{65}$$

Fig. 4. The rescaled radial component of the mean charge current. Namely, $\mathcal{J} \cdot \hat{r} \times 10^4 q^{-1} m^{-3}$ at $mt = 40$. The black line comes from (62), whereas the blue one is obtained from (59). The inset magnifies the shock wave discontinuity.

The first two of these expressions can be easily read off (60) and (61) while the last one has been obtained from (62) with the help of

$$\int\limits_{0}^{mt} dx \mathrm{J}_0\left(\sqrt{(mt)^2 - x^2}\right) = \sin(mt), \tag{66}$$

see formula 6.517 listed in [11].

Near $r = 0$ the following expressions describe the quantities of interest

$$\mathcal{E}(t, \boldsymbol{r}) = -\frac{qm^3 \hat{r}}{12\pi} F(mt) r + O\left(r^3\right), \tag{67}$$

$$\mathcal{J}^0(t, \boldsymbol{r}) = -\frac{qm^3}{4\pi} F(mt) + O\left(r^2\right), \tag{68}$$

$$\mathcal{J}(t, \boldsymbol{r}) = -\frac{qm^4 \hat{r}}{24\pi} [\mathrm{J}_0(mt) + \mathrm{J}_2(mt)] r + O\left(r^3\right), \tag{69}$$

where

$$F(x) = 1 + \mathrm{J}_1(x) - x\mathrm{J}_0(x) - \frac{\pi x}{2} \mathrm{J}_1(x)\mathrm{H}_0(x) + \frac{\pi x}{2} \mathrm{J}_0(x)\mathrm{H}_1(x) \tag{70}$$

with H_n representing the Struve function of order n (the last three terms of (70) correspond to $-\int_0^x dx \mathrm{J}_0(x)$; see expression 6.511.6 listed in [11]).

The short-time dynamics of (67)–(69) can be grasped by taking a look at Fig. 5. The long-time dynamics of (67)–(69) is encoded in the following formulas that can be derived with the help of [11]

$$F(x) = \sqrt{\frac{2}{\pi x^3}} \sin\left(x + \frac{\pi}{4}\right) + O\left(x^{-5/2}\right), \tag{71}$$

$$\mathrm{J}_0(x) + \mathrm{J}_2(x) = 2\sqrt{\frac{2}{\pi x^3}} \sin\left(x - \frac{\pi}{4}\right) + O\left(x^{-5/2}\right). \tag{72}$$
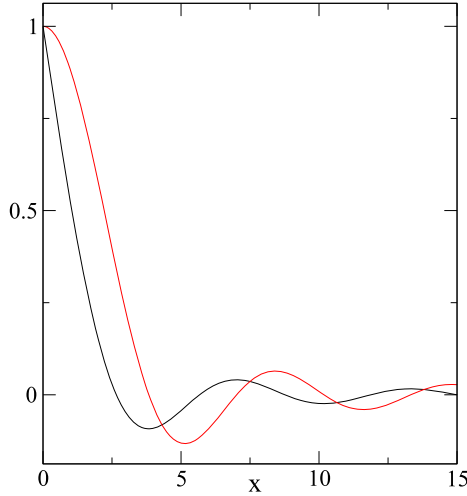
Fig. 5. The black line shows (70), whereas the red one depicts $J_0(x) + J_2(x)$. Asymptotic expressions (71) and (72) are on the plotted scale indistinguishable from the exact results for $x > 10$.

These expressions show that (67)–(69) exhibit damped oscillations for $t \to \infty$, which are somewhat reminiscent of the dynamics seen in the studies of quantum transients [12]. The difference between the arguments of the sine functions in (71) and (72) can be understood by considering the dynamics of the charge contained in a tiny sphere around the point $r = 0$. The decrease (increase) of such a charge is caused by the outward (inward) orientation of the charge current, which the $\pi/2$ phase shift guarantees.

Finally, we compute the total charge stored in the ball of radius t^-, which is given by

$$\mathcal{Q}(t, r < t) = \lim_{r \to t^-} \int d\mathbf{S}(\mathbf{r}) \cdot \boldsymbol{\mathcal{E}}(t, \mathbf{r}) = q\cos(mt) - q\exp(-mt)(1 + mt). \tag{73}$$

By combining this result with (57), we see that

$$\mathcal{Q}(t, r < t) + \mathcal{Q}(t, r > t) = \mathcal{Q}(t). \tag{74}$$

5.4. Perpetual dynamics: from escaping to collapsing evolution

Expressions (35), (36), and (37) exhibit the following time-reversal (anti)symmetry

$$\boldsymbol{\mathcal{E}}(-t, \mathbf{r}) = \boldsymbol{\mathcal{E}}(t, \mathbf{r}), \tag{75}$$

$$\mathcal{J}^0(-t, r) = \mathcal{J}^0(t, r), \tag{76}$$

$$\boldsymbol{\mathcal{J}}(-t, \mathbf{r}) = -\boldsymbol{\mathcal{J}}(t, \mathbf{r}). \tag{77}$$

As a result of that, by solving the dynamics of the mean electric field, charge density, and charge current for $t > 0$, one actually gets the above quantities also for the times $t < 0$ under the following condition. Namely, one has to assume that the Schrödinger picture state of the system at such times is given by the action of the operator $\exp(-iHt)$ onto (28), where H is given by (15b).

In particular, in the context of the specific studies discussed in section 5, such an extension of the dynamics to the domain $t < 0$ leads to the following observations. We could say that for

$t : -\infty \to 0^-$ there is a collapsing (incoming) regularized Coulomb field in the studied problem. At $t = 0$ the regularized Coulomb field is fully formed and the state of the system is given by (28) combined with (38), (42), and (43). Then, for $t : 0^+ \to \infty$ the dynamics of the escaping (outgoing) regularized Coulomb field is seen in the analyzed problem.

Finally, we note that the results discussed in this work are markedly distinct from topological [13] and non-topological [14] soliton solutions, despite the fact that the "charge" profoundly impacts both our and the soliton considerations.

6. Further illustration of periodic charge oscillations

We discuss here further concrete theoretical illustration of periodic charge oscillations. For this purpose, we briefly extend the studies from section 5 by considering

$$f(\omega_k) = \left(\frac{m}{\varepsilon_k}\right)^\gamma, \tag{78}$$

where

$$\gamma = 4, 6, 8, \cdots \tag{79}$$

for the technical reason mentioned below (D.1). The following comments are in order now.

First, by repeating the calculations from the beginning of section 5, we find that now

$$1 = \alpha^2 + \beta^2 \frac{e^2}{8\pi^{3/2}} \frac{\Gamma(\gamma - 1)}{\Gamma(\gamma - 1/2)}, \tag{80}$$

$$\mathcal{H} = \beta^2 m \frac{e^2}{8\pi^{3/2}} \frac{\Gamma(\gamma - 3/2)}{\Gamma(\gamma - 1)}, \tag{81}$$

the amplitude of periodic charge oscillations is upper bounded by

$$\sqrt{2\pi^{3/2} \frac{\Gamma(\gamma - 1/2)}{\Gamma(\gamma - 1)}}, \tag{82}$$

and α and β are given by (42) and (43) with π replaced by (82).

Second, the electric field potential now reads

$$\phi(t, r; \gamma) = \frac{q}{2\pi^2 r} \int\limits_0^\infty d\omega_k \left(\frac{m}{\varepsilon_k}\right)^\gamma \frac{\sin(\omega_k r)}{\omega_k} \cos(\varepsilon_k t). \tag{83}$$

It turns out that it is smoother than $\phi(t, r)$ studied in section 5. In particular, it follows from the discussion in appendix E that (83) and all its derivatives up to the order $\gamma - 2$ are continuous. This implies that (34) and (35) are equivalent, the equalities in (36) and (37) hold, and the mean electric field and 4-current are continuous at $r = t$. Despite all that, $\phi(t, r; \gamma)$ is non-analytic (e.g. it can be inferred from appendix E.1 that at least some derivatives of (83) of the order γ are undefined at $r = t$). In other words, there is a shock wave here just as in section 5, a more gentle one, however.

Third, we would like to mention one more consequence of the above-specified smoothness of $\phi(t, r; \gamma)$. Namely, as can be inferred from (E.13), $r\phi(t, r; \gamma)$ satisfies the $1 + 1$ dimensional Klein-Gordon equation

$$\left(\frac{\partial^2}{\partial r^2} - \frac{\partial^2}{\partial t^2}\right)\left[r\phi(t,r;\gamma)\right] = m^2 r\phi(t,r;\gamma), \tag{84}$$

which places the results discussed in this section in a broader context.

Fourth, we find that for $r \geq t > 0$

$$\phi(t,r;\gamma) = q\frac{\cos(mt) - P_\gamma(mr, mt)\exp(-mr)}{4\pi r}, \tag{85}$$

$$\boldsymbol{\mathcal{E}}(t,\boldsymbol{r};\gamma) = \frac{q\hat{\boldsymbol{r}}}{4\pi r^2}\cos(mt) - \frac{q\hat{\boldsymbol{r}}\exp(-mr)}{4\pi r^2}(1 + mr - r\partial_r)P_\gamma(mr, mt), \tag{86}$$

$$\mathcal{J}^0(t,r;\gamma) = \frac{q\exp(-mr)}{4\pi r}(m - \partial_r)^2 P_\gamma(mr, mt), \tag{87}$$

$$\boldsymbol{\mathcal{J}}(t,\boldsymbol{r};\gamma) = \frac{qm\hat{\boldsymbol{r}}}{4\pi r^2}\sin(mt) + \frac{q\hat{\boldsymbol{r}}\exp(-mr)}{4\pi r^2}(1 + mr - r\partial_r)\frac{\partial}{\partial t}P_\gamma(mr, mt), \tag{88}$$

where P_γ is a finite-degree polynomial of both arguments (see appendix D, where the recipe for the generation of these polynomials is provided along with some explicit results for small values of γ). We will now briefly comment upon these results.

Expressions (85) and (86) manifestly encode the periodic charge oscillations and it is immediately evident from them that (56) also holds in the discussed case. Moreover, they illustrate that the short-range contribution to the electric field potential, and so also to the mean electric field, does not have to be static in the studied region of space. Mean charge density (87) is qualitatively the same as (58), both quantities are negligible in the long-distance limit. Finally, apart from the exponentially small in r correction, mean charge current (88) is the same as (59).

7. Relativity-related issues

Two features of the solutions discussed in sections 5 and 6 may seem to be a bit counterintuitive if one takes into account that the Lorentz invariant theory is studied in this paper.

First, there is the question of how the periodic oscillations of the long-range component of the mean electric field can simultaneously happen at arbitrarily large distances. Second, there is the question of how the charge could periodically disappear and reappear as if it would be instantly transferred all the way to spatial infinity. We will discuss these issues below.

7.1. Long-range oscillations of electric field

The first terms in (55) and (86) have a curious property. Namely, they describe global, i.e. simultaneous for all $r > t$, oscillations of the Coulomb field. At first sight, such oscillations may look as if they were caused by the infinite propagation speed of some signal. However, their presence does not contradict special theory of relativity because the Coulomb field, at every point in the $r > t$ region, oscillates in a predefined manner.

We note that qualitatively the same effect can be observed in the setup composed of harmonic oscillators, say identical spring-mass systems depicted in Fig. 6. Namely, one can place them along some line, take each one of them out of its equilibrium position in the direction perpendicular to that line, and release them at one and the same time moment in their common rest frame (the last step can be always done by equipping each oscillator with a synchronized clock and a mechanism automatically starting the oscillations at the predefined time instant). By properly choosing the initial displacement of each oscillator, the mechanical model of the simultaneous Coulomb field oscillations can be obtained.
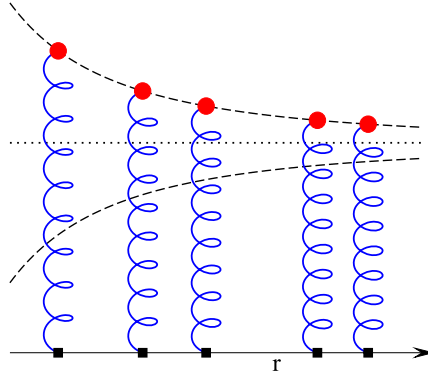
Fig. 6. The schematic illustration of the mechanical model of the simultaneous Coulomb field oscillations. The springs are depicted in blue. The oscillating masses are presented as red dots. The black dotted line goes through the equilibrium positions of the oscillating masses (oscillations take place in the vertical direction). The initial displacements of the masses from their equilibrium positions are chosen along the upper black dashed line, which is assumed to be described by A/r^2 (r is the position of each spring along the horizontal axis, A is a positive constant). As the lower dashed line depicts $-A/r^2$, the masses oscillate between the two dashed lines. If the angular frequency of these oscillations is equal to ω, then the displacements of the masses are given by $A\cos(\omega t)/r^2$, which is qualitatively the same as the formula describing the radial component of the periodically oscillating Coulomb field in (55) and (86).

7.2. Charge transport

For the sake of simplicity and definiteness, we will focus here on the discussion of the dynamics carefully worked out in section 5 (the results presented in section 6 can be similarly commented upon). To begin, we would like to stress that the periodic variation of the total charge has nothing to do with the discontinuity of the mean 4-current captured by (51) and (52). In other words, the periodically oscillating charge is not appearing or disappearing because it comes in and out of the "shock portal". For example, this is evident from the discussion in section 6, where exactly the same periodic oscillations of the total charge happen in the presence of the continuous mean 4-current.

Having said all that, we turn our attention to mean charge current (59), computing its flux through the sphere of the radius $R > t$

$$\int d\boldsymbol{S}(\boldsymbol{R}) \cdot \boldsymbol{\mathcal{J}}(t, \boldsymbol{R}) = qm\sin(mt). \tag{89}$$

Since this result is independent of R, it suggests that the periodically oscillating charge outflows (inflows) to (from) spatial infinity without being accumulated anywhere in the $r > t$ region. As this happens, the charge inside the $r < t$ region accordingly decreases (increases).

However, the claim that the periodically oscillating charge flows through the region $r > t$ could be confusing because according to (58) such a charge does not seem to be ever present there.[4] This remark suggests that we have a paradox here, the empty hose paradox so to speak, whose illustration is presented in Fig. 7. It is our opinion that its explanation may be the following.

---

[4] Charge density (58) comes from the time-independent Debye component of mean electric field (55), which has nothing to do with periodically oscillating flux (89). The time-dependent Coulomb component of mean electric field (55) makes (89) non-zero, but it does *not* contribute to charge density (58).
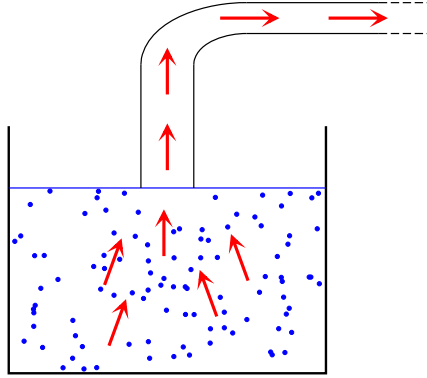
Fig. 7. The schematic hydrodynamic illustration of the empty hose paradox. The container is filled with the fluid depicted by blue dots. The fluid either leaves or enters the container via the hose. Such a situation is paradoxical because the density of the fluid, unlike its velocity field depicted by red arrows, vanishes inside the hose. In the Proca theory context, the container represents the $r < t$ region, the hose represents the $r > t$ region, and the fluid stands for the periodically oscillating charge.

To begin, we note that $\mathcal{J}^0$ can be locally either positive or negative and consider at some time $t > 0$ two spheres having radiuses R and $R + dR$, where $R > t$ and dR is infinitesimally small. We envision the following process. The charge outflowing via the larger sphere between the times t and $t + dt$ leaves behind the spheres the charge $-q \sin(mt) m \, dt$, which is simultaneously "neutralized" by the charge $q \sin(mt) m \, dt$ flowing into the area between the spheres via the smaller sphere. In other words, the very fact that the charge density can be either positive or negative creates the opportunity that at any time moment the mean charge between the spheres can be equal to zero. By considering the series of spheres with progressively larger radiuses, $t + dR$, $t + 2dR$, $t + 3dR$, $\cdots$, we can see how the charge $q \sin(mt) m \, dt$ may disappear from the system between time instants t and $t + dt$.

8. Summary

We have studied the dynamics of normalizable finite-energy charged states in the Proca theory. Two characteristic features have been observed in the course of these investigations.

First, we have found that at large distances the mean electric field in the studied states is given by the Coulomb field that is periodically oscillating in the time domain. On the one hand, such a result explains the periodic charge oscillations. On the other hand, it leads to the relativity-related questions that we have discussed.

Second, we have found that there is a genuine shock wave propagating in the studied states. Its presence breaks analyticity of the mean electric field and the related quantities such as the mean charge density and current.

We hope that these and other results that we have presented provide solid evidence that the studies of the dynamics of charged states in the Proca theory constitute a well-defined mathematical problem, where elegant analytical results can be obtained.

If we now turn our attention to the question of whether the discussed results can be experimentally approached, the situation is problematic for the following two reasons.

First, the causality considerations exclude the possibility of the experimental preparation of charged states. Still, one may consider the perpetual evolution scenario that we have proposed, in

which the charged states are eternally evolving across the Universe as opposed to being created in the laboratory.

Second, there is the question of what stable particle could represent the massive vector boson described by the Proca theory. In this respect, one may consider the possibility that photons may have a non-zero mass (this issue is related to the experimental studies that have been carried out for over two centuries so far [2,15]). In fact, there exist various upper bounds on the photon mass ranging e.g. from 10^{-49} kg to 10^{-54} kg [2]. Upon substitution of such values into (24), one gets an intriguing lower bound on the oscillation period of the Coulomb component of the mean electric field in charged states: 7×10^{-2} s to 7×10^3 s.

All in all, we see this work as being mainly of theoretical interest at the moment. It is our opinion that further research along these lines could lead to the in-depth understanding of the charged sectors of Proca and similar theories possessing a non-trivial infrared structure.

CRediT authorship contribution statement

All work on this article has been done by its only author: Bogdan Damski.

Declaration of competing interest

The author declares that he has no known competing financial interests or personal relationships that could have appeared to influence the work reported in this paper.

Data availability

No data was used for the research described in the article.

Acknowledgements

Appendix A. Conventions

We use the metric tensor $\text{diag}(+ - - -)$. Greek and Latin indices of tensors take values 0, 1, 2, 3 and 1, 2, 3, respectively. 3-vectors are written in bold, e.g. $x = (x^\mu) = (x^0, \boldsymbol{x})$.

We adopt the Heaviside-Lorentz system of units and set $\hbar = c = 1$. Hyperbolic sin, cos, tan, and cot are denoted as sh, ch, th, and cth, respectively. $\partial_t = \partial/\partial t$, $\partial_r = \partial/\partial r$, $\mathbb{N}_0 = \{0, 1, 2, \cdots\}$, α^+ (α^-) denotes the quantity that is infinitesimally larger (smaller) than α, and the hermitian conjugation is represented by h.c.

Appendix B. Integral from expression (44)

We evaluate here

$$I(a, b) = \int_0^\infty dx \, \frac{\sin[a \operatorname{sh}(x)] \cos[b \operatorname{ch}(x)]}{\operatorname{sh}(x) \operatorname{ch}(x)} \tag{B.1}$$

representing the integral from (44) after the following change of variables

$$\omega_k = m \operatorname{sh}(x), \tag{B.2a}$$

$$mr = a, \ mt = b. \tag{B.2b}$$

We will assume below that $a > 0$, $b \geq 0$.

To proceed, we will be computing

$$I_\pm(C) = \int_C dz \, \frac{\exp[ia \operatorname{sh}(z) \pm ib \operatorname{ch}(z)]}{\operatorname{sh}(z) \operatorname{ch}(z)} \tag{B.3}$$

over the contours depicted in Figs. 8 and 9. We have chosen their shapes in a standard way, taking into account the fact that the integrand has simple poles at integer and half-integer multiples of $i\pi$.

B.1. $a \geq b > 0$

The goal here is to prove that for $a \geq b > 0$

$$I(a, b) = \frac{\pi}{2} \left[\cos(b) - \exp(-a) \right]. \tag{B.4}$$

The integral $I_+(C)$ is done over the contour from Fig. 8. Proceeding in a standard way, we get

$$\fint dx \, \frac{\sin[a \operatorname{sh}(x) + b \operatorname{ch}(x)]}{\operatorname{sh}(x) \operatorname{ch}(x)} = \pi \cos(b) - \pi \exp(-a), \tag{B.5}$$

where the limits of $R \to \infty$ and $\varepsilon \to 0^+$ have been taken and $\fint$ stands for the Cauchy principal value

$$\fint = \lim_{\varepsilon \to 0^+} \left(\int_{-\infty}^{-\varepsilon} + \int_{\varepsilon}^{\infty} \right). \tag{B.6}$$

The left-hand side of (B.5) comes from integration over horizontal segments. The right-hand side of (B.5), besides the $-\pi \exp(-a)$ pole contribution, comes from integration over semi-circular segments.

The vertical segments do not contribute to (B.5) for the following reasons. At $z = -R + iy$,

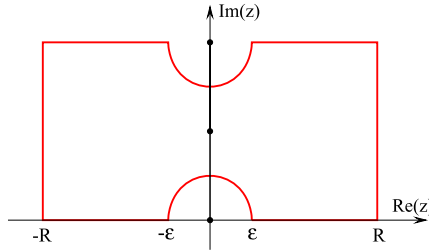$$\left| \frac{1}{\operatorname{sh}(z) \operatorname{ch}(z)} \right| = O(\exp(-2R)), \tag{B.7}$$

Fig. 8. Integration contour. Its horizontal segments are at $\mathrm{Im}(z) = 0, \pi$. The curved segments are semi-circular with radius ε. The poles of the integrand are depicted by the dots (they are located at $z = 0, i\pi/2, i\pi$).

$$|\exp[ia\,\mathrm{sh}(z) + ib\,\mathrm{ch}(z)]| = \exp\left(-\frac{a-b}{2}\sin(y)\exp(R) + \epsilon(a,b)\right), \tag{B.8a}$$

$$\epsilon(a,b) = -\frac{a+b}{2}\sin(y)\exp(-R) = O(\exp(-R)), \tag{B.8b}$$

and so the integrand vanishes in the $R \to \infty$ limit for any fixed

$$0 \le y \le \pi \tag{B.9}$$

being of interest here. Note that it is so because the $a \ge b$ case is considered. The same conclusion applies to the vertical segment parameterized by $z = R + iy$ because (B.7) still holds,

$$|\exp[ia\,\mathrm{sh}(z) + ib\,\mathrm{ch}(z)]| = \exp\left(-\frac{a+b}{2}\sin(y)\exp(R) + \epsilon(a,-b)\right), \tag{B.10}$$

and $a + b > 0$.

The integral $I_-(C)$ is also done over the contour from Fig. 8. In very much the same way as above, it leads to

$$\fint dx\,\frac{\sin[a\,\mathrm{sh}(x) - b\,\mathrm{ch}(x)]}{\mathrm{sh}(x)\,\mathrm{ch}(x)} = \pi\cos(b) - \pi\exp(-a), \tag{B.11}$$

which immediately follows from the $x \to -x$ change of the integration variable in (B.5). By combining (B.5) and (B.11), (B.4) can be established.

B.2. $b > a > 0$

It will be first argued here that for $b > a > 0$

$$I(a,b) = \frac{\pi}{2}\,\mathrm{sh}(a) - \int_0^{\pi/2} dx\,\frac{\mathrm{sh}[a\cos(x)]\sin[b\sin(x)]}{\sin(x)\cos(x)} \tag{B.12}$$

and then it will be shown that

$$I(a,b) = \frac{\pi}{2}[\cos(a) - \exp(-a)] - \frac{\pi}{2}\int_a^b dy\int_0^a dx\,\mathrm{J}_0\left(\sqrt{y^2 - x^2}\right). \tag{B.13}$$

These equations trigger the following comment.

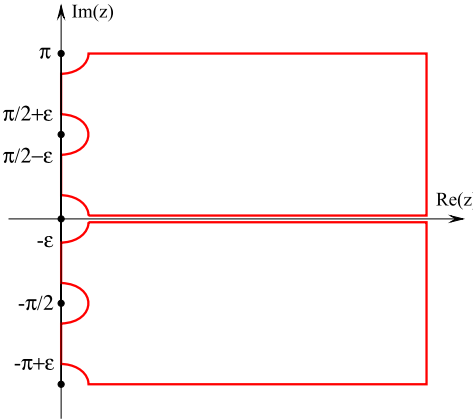Fig. 9. Two integration contours. Their horizontal and vertical segments are at $\text{Im}(z) = -\pi, 0, \pi$ and $\text{Re}(z) = 0, R$, respectively. The curved segments, half- and quarter-circular, have radius ε. They go around the poles of the integrand, which are depicted by black dots. The lower contour is the mirror image of the upper one.

We are unaware of the closed-form expressions for the integrals in (B.12) and (B.13). Nonetheless, the above formulas are arguably more useful than (B.1). It is so because their derivatives with respect to a and b can be easily computed and they are manifestly finite. This is particularly clearly seen from (B.12), where it is evident that the integrand and all its derivatives with respect to a and b are defined and continuous,[5] which in the case of the *proper* integral is basically all one needs to know to be able to take the derivatives under the integral symbol.[6] By contrast, the differentiation of (B.1) is more complicated because we deal in such a case with an *improper* integral over an unbounded interval.

We start the discussion of the derivation of (B.12) with the computation of $I_+(C)$ over the upper contour in Fig. 9. Note that the contour from Fig. 8 cannot be now used for the evaluation of $I_+(C)$ because the integrand on its vertical segment at $\text{Re}(z) = -R$ quickly grows in the $R \to \infty$ limit when $b > a$, which is seen from (B.8).

We proceed similarly as in section B.1. Introducing

$$\Upsilon_{\pm}(\varepsilon) = \int_{\varepsilon}^{\infty} dx \, \frac{\sin[a \, \text{sh}(x) \pm b \, \text{ch}(x)]}{\text{sh}(x) \, \text{ch}(x)}$$

$$\pm \frac{i}{2} \left(\int_{\varepsilon}^{\pi/2-\varepsilon} + \int_{\pi/2+\varepsilon}^{\pi-\varepsilon} \right) dx \, \frac{\exp[\mp a \sin(x) + ib \cos(x)]}{\sin(x) \cos(x)}, \qquad (\text{B.14})$$

we arrive at

$$\lim_{\varepsilon \to 0^+} \Upsilon_+(\varepsilon) = \frac{\pi}{2} \left[\cos(b) - \exp(-a) \right]. \qquad (\text{B.15})$$

---

[5] It should be understood that $\sin[b \sin(x)]/\sin(x) = b \left(1 - b^2 \sin^2(x)/3! + \cdots \right)$ near and at $x = 0$. Similarly, $\text{sh}[a \cos(x)]/\cos(x) = a \left(1 + a^2 \cos^2(x)/3! + \cdots \right)$ near and at $x = \pi/2$.

[6] The issue of interchanging derivatives and integrals is discussed in numerous textbooks (see e.g. [16]). The particularly comprehensive presentation of this topic can be found in Polish in [17].

The first term in (B.14) comes from integration over the horizontal segments. The rest of (B.14) comes from integration over the vertical segments at $\mathrm{Re}(z) = 0$. The right-hand side of (B.15) comes from integration over semi- and quarter-circular segments. The vertical segment at $\mathrm{Re}(z) = R$ does not contribute, which is seen from (B.10). The limit of $R \to \infty$ has been taken in the above expressions.

Next, we integrate $I_-(C)$ over the lower contour in Fig. 9. The key observation here is that integration over the vertical segment at $\mathrm{Re}(z) = R$ does not contribute. It is so because for $z = R - \mathrm{i}y$, where again (B.9) is used, we have (B.7) and

$$|\exp[\mathrm{i}a\,\mathrm{sh}(z) - \mathrm{i}b\,\mathrm{ch}(z)]| = \exp\left(-\frac{b-a}{2}\sin(y)\exp(R) - \epsilon(a,b)\right). \tag{B.16}$$

Thereby, the integrand vanishes in the $R \to \infty$ limit for $b > a$ considered now. Proceeding similarly as above, we arrive at

$$\lim_{\varepsilon \to 0^+} \Upsilon_-(\varepsilon) = \frac{\pi}{2}\left[\exp(a) - \cos(b)\right]. \tag{B.17}$$

By combining (B.15) and (B.17), (B.12) can be established.

Result (B.12) can be used for expressing the integral of interest in terms of the Bessel function. Namely, denoting the integral in (B.12) by $\tilde{I}(a,b)$, we find that

$$\frac{\partial^2}{\partial a\,\partial b}\tilde{I}(a,b) = \frac{\pi}{2}\mathrm{J}_0\left(\sqrt{b^2-a^2}\right) \tag{B.18}$$

after taking into account formula 3.996.3 of [11]

$$\int_0^{\pi/2} dx\,\mathrm{ch}[a\cos(x)]\cos[b\sin(x)] = \frac{\pi}{2}\mathrm{J}_0\left(\sqrt{b^2-a^2}\right). \tag{B.19}$$

Solving (B.18) with the boundary conditions $\lim_{a\to 0}\tilde{I}(a,b) = \lim_{b\to 0}\tilde{I}(a,b) = 0$, we get

$$\tilde{I}(a,b) = \frac{\pi}{2}\int_0^a dx \int_0^b dy\,\mathrm{J}_0\left(\sqrt{y^2-x^2}\right), \tag{B.20}$$

where it has to be understood that for $y < x$ we have $\mathrm{J}_0\left(\sqrt{y^2-x^2}\right) = \mathrm{I}_0\left(\sqrt{x^2-y^2}\right)$ with I_n representing the modified Bessel function of the first kind of order n. Simple manipulations, involving the following variant of (66)

$$\int_0^x dy\,\mathrm{I}_0\left(\sqrt{x^2-y^2}\right) = \mathrm{sh}(x), \tag{B.21}$$

lead to (B.13). Another potentially useful representation of (B.12) is given by (C.21).

B.3. $a > b = 0$

One may easily verify with the help of appendix B.1 that

$$I(a,0) = \frac{\pi}{2}\left[1 - \exp(-a)\right] \text{ for } a > 0. \tag{B.22}$$

B.4. From continuity to discontinuity across $a = b > 0$

With the help of the above discussed results, we find that

$$\lim_{a \to b^-} I(a, b) = \lim_{a \to b^+} I(a, b), \tag{B.23}$$

$$\lim_{a \to b^-} \frac{\partial}{\partial a} I(a, b) = \lim_{a \to b^+} \frac{\partial}{\partial a} I(a, b), \tag{B.24}$$

$$\lim_{a \to b^-} \frac{\partial}{\partial b} I(a, b) = \lim_{a \to b^+} \frac{\partial}{\partial b} I(a, b), \tag{B.25}$$

$$\lim_{a \to b^-} \frac{\partial^2}{\partial a^2} I(a, b) = \frac{\pi}{2} + \lim_{a \to b^+} \frac{\partial^2}{\partial a^2} I(a, b), \tag{B.26}$$

$$\lim_{a \to b^-} \frac{\partial^2}{\partial a \partial b} I(a, b) = -\frac{\pi}{2} + \lim_{a \to b^+} \frac{\partial^2}{\partial a \partial b} I(a, b), \tag{B.27}$$

$$\lim_{a \to b^-} \frac{\partial^2}{\partial b^2} I(a, b) = \frac{\pi}{2} + \lim_{a \to b^+} \frac{\partial^2}{\partial b^2} I(a, b). \tag{B.28}$$

Appendix C. Integral from expression (44): differentiation under the integral sign

We introduce the following notation

$$I_{\alpha\beta}(a, b) = \int_0^\infty dx \, \frac{\partial^\alpha}{\partial a^\alpha} \frac{\partial^\beta}{\partial b^\beta} \frac{\sin[a \operatorname{sh}(x)] \cos[b \operatorname{ch}(x)]}{\operatorname{sh}(x) \operatorname{ch}(x)}, \tag{C.1}$$

where $\alpha, \beta \in \mathbb{N}_0$ and $I_{\alpha\beta}$ should not be confused with the modified Bessel function of the first kind I_n. The goal here is to compute $I_{\alpha\beta}(a, b)$ for $1 \le \alpha + \beta \le 2$ and to compare it to

$$\partial_a^\alpha \partial_b^\beta I(a, b) = \frac{\partial^\alpha}{\partial a^\alpha} \frac{\partial^\beta}{\partial b^\beta} \int_0^\infty dx \frac{\sin[a \operatorname{sh}(x)] \cos[b \operatorname{ch}(x)]}{\operatorname{sh}(x) \operatorname{ch}(x)}, \tag{C.2}$$

which can be obtained from the results presented in appendix B. This will be done under the tacit assumption that $a, b > 0$.

Whenever the order of differentiation and integration does not matter, i.e. when

$$\left[\frac{\partial^\alpha}{\partial a^\alpha} \frac{\partial^\beta}{\partial b^\beta}, \int_0^\infty dx \right] = 0 \tag{C.3}$$

in the studied problem, we will have $I_{\alpha\beta}(a, b) = \partial_a^\alpha \partial_b^\beta I(a, b)$. The formal determination of when it happens, which would reduce the number of integrals evaluated in this section, is not so trivial because we deal here with improper integrals over an unbounded interval.[7] Therefore, as far as we see it, the easiest way to proceed here is to do a direct, i.e. brute force, evaluation of $I_{\alpha\beta}(a, b)$.

---

[7] The term formal refers here to "theorem-based" considerations, where no explicit integral evaluations are carried out. The considerations of such a type can be found in appendix E, but as they stand they are not sophisticated enough to yield useful information in the context of the studies discussed in appendix C.

The comparison of such obtained results to $\partial_a^\alpha \partial_b^\beta I(a, b)$ could be then straightforwardly done [see e.g. the comment below (B.13)].

The results reported below come from the evaluations of

$$\int_C dz f(z) \exp[ia\,\text{sh}(z) \pm ib\,\text{ch}(z)], \tag{C.4}$$

which proceed similarly as the carefully discussed calculations reported in appendices B.1 and B.2. Thus, we will not dwell on the technical details of such computations. We will, however, briefly comment upon two issues.

First, (C.4) will be evaluated over the contours from Figs. 8 and 9 subjected to small alterations (replacements of half- and quarter-circular segments by line segments in the absence of poles). The contour(s) from Fig. 8 (Fig. 9) will be re-used for $a \geq b$ ($b > a$).

Second, $f(z)$ will be given by $1/\text{ch}(z)$, $1/\text{sh}(z)$, $\text{th}(z)$, 1, and $\text{cth}(z)$ during the evaluation of (C.5), (C.7), (C.11), (C.13), and (C.15), respectively. This means that in the last three cases $|f(\pm R + iy)| \to 1$ in the $R \to \infty$ limit when $0 \leq y \leq \pi$. This is of crucial importance for the case of $a = b$. Namely, it implies that for $a = b$ the vertical segment of the contour at $\text{Re}(z) = -R$ ($\text{Re}(z) = R$) will contribute to integral (C.4) when the $+$ ($-$) sign will be chosen. This fact stands behind the $\pi/4$ shift in (C.12b), (C.14b), and (C.16b).

C.1. First order derivatives

We have found that

$$I_{10}(a, b) = \int_0^\infty dx \frac{\cos[a\,\text{sh}(x)]\cos[b\,\text{ch}(x)]}{\text{ch}(x)} \tag{C.5}$$

is equal to

$$\frac{\pi}{2}\exp(-a) \text{ for } a \geq b, \tag{C.6a}$$

$$\frac{\pi}{2}\exp(-a) - \frac{\pi}{2}\int_a^b dx J_0\left(\sqrt{x^2 - a^2}\right) \text{ for } b > a. \tag{C.6b}$$

Moreover, we have found that

$$I_{01}(a, b) = -\int_0^\infty dx \frac{\sin[a\,\text{sh}(x)]\sin[b\,\text{ch}(x)]}{\text{sh}(x)} \tag{C.7}$$

is equal to

$$-\frac{\pi}{2}\sin(b) \text{ for } a \geq b, \tag{C.8a}$$

$$-\frac{\pi}{2}\sin(b) + \frac{\pi}{2}\int_a^b dx J_0\left(\sqrt{b^2 - x^2}\right) \text{ for } b > a. \tag{C.8b}$$

As can be easily checked, (C.6) and (C.8) agree everywhere with $\partial_a I(a, b)$ and $\partial_b I(a, b)$, respectively. Note that we refer here to $\partial_a I(a, b)$ and $\partial_b I(a, b)$ obtained via differentiation of

(B.4) and either (B.12) or (B.13). We mention in passing that despite the piecewise structure of the expression for $I(a, b)$,

$$\partial_a I(b, b) = \lim_{\epsilon \to 0} \frac{I(b + \epsilon, b) - I(b, b)}{\epsilon} \tag{C.9}$$

and

$$\partial_b I(b, b) = \lim_{\epsilon \to 0} \frac{I(b, b + \epsilon) - I(b, b)}{\epsilon} \tag{C.10}$$

are well defined. As there are no surprises here, we shall not discuss these findings any further.

C.2. Second order derivatives

We have found that

$$I_{20}(a, b) = -\int_0^\infty dx \, \text{th}(x) \sin[a \, \text{sh}(x)] \cos[b \, \text{ch}(x)] \tag{C.11}$$

is equal to

$$-\frac{\pi}{2} \exp(-a) \text{ for } a > b, \tag{C.12a}$$

$$-\frac{\pi}{2} \exp(-a) + \frac{\pi}{4} \text{ for } a = b, \tag{C.12b}$$

$$-\frac{\pi}{2} \exp(-a) + \frac{\pi}{2} - \frac{a\pi}{2} \int_a^b dx \frac{J_1\left(\sqrt{x^2 - a^2}\right)}{\sqrt{x^2 - a^2}} \text{ for } b > a. \tag{C.12c}$$

Then, we have found that

$$I_{11}(a, b) = -\int_0^\infty dx \cos[a \, \text{sh}(x)] \sin[b \, \text{ch}(x)] \tag{C.13}$$

is equal to

$$0 \text{ for } a > b, \tag{C.14a}$$

$$-\frac{\pi}{4} \text{ for } a = b, \tag{C.14b}$$

$$-\frac{\pi}{2} J_0\left(\sqrt{b^2 - a^2}\right) \text{ for } b > a. \tag{C.14c}$$

Finally, we have found that

$$I_{02}(a, b) = -\int_0^\infty dx \, \text{cth}(x) \sin[a \, \text{sh}(x)] \cos[b \, \text{ch}(x)] \tag{C.15}$$

is equal to

$$-\frac{\pi}{2}\cos(b) \text{ for } a > b, \tag{C.16a}$$

$$-\frac{\pi}{2}\cos(b) + \frac{\pi}{4} \text{ for } a = b, \tag{C.16b}$$

$$-\frac{\pi}{2}\cos(b) + \frac{\pi}{2} - \frac{b\pi}{2}\int_a^b dx \frac{J_1\left(\sqrt{b^2 - x^2}\right)}{\sqrt{b^2 - x^2}} \text{ for } b > a. \tag{C.16c}$$

Simple calculations show that everywhere except at $a = b$ (C.12), (C.14), and (C.16) are equal to $\partial_a^2 I(a, b)$, $\partial_a \partial_b I(a, b)$, and $\partial_b^2 I(a, b)$, respectively. Note that we refer here to $\partial_a^2 I(a, b)$, $\partial_a \partial_b I(a, b)$, and $\partial_b^2 I(a, b)$ obtained via differentiation of (B.4) and either (B.12) or (B.13). At $a = b$, we find that $\partial_a^2 I(a, b)$, $\partial_a \partial_b I(a, b)$, and $\partial_b^2 I(a, b)$ are undefined, which is in stark contrast to what we have in (C.12b), (C.14b), and (C.16b). This is seen from the fact that the limits

$$\lim_{\epsilon \to 0} \frac{\partial_a I(b + \epsilon, b) - \partial_a I(b, b)}{\epsilon}, \tag{C.17}$$

$$\lim_{\epsilon \to 0} \frac{\partial_b I(b + \epsilon, b) - \partial_b I(b, b)}{\epsilon}, \tag{C.18}$$

$$\lim_{\epsilon \to 0} \frac{\partial_b I(b, b + \epsilon) - \partial_b I(b, b)}{\epsilon} \tag{C.19}$$

do not exist.

Finally, we would like to mention the following identity

$$I_{20}(a, b) - I_{02}(a, b) = I(a, b). \tag{C.20}$$

After putting (C.12c) and (C.16c) into it, the new representation of (B.12) is obtained

$$\frac{\pi}{2}\left[\cos(b) - \exp(-a)\right] + \frac{\pi}{2}\int_a^b dx \left(b\frac{J_1\left(\sqrt{b^2 - x^2}\right)}{\sqrt{b^2 - x^2}} - a\frac{J_1\left(\sqrt{x^2 - a^2}\right)}{\sqrt{x^2 - a^2}}\right). \tag{C.21}$$

Appendix D. Integral from expression (83): insights relevant for periodic charge oscillations

We briefly discuss below

$$I(a, b; \gamma) = \int_0^\infty dx \frac{\sin[a \operatorname{sh}(x)] \cos[b \operatorname{ch}(x)]}{\operatorname{sh}(x) \operatorname{ch}^{\gamma-1}(x)} \tag{D.1}$$

representing the integral from (83) under mapping (B.2). We focus here on the $a \geq b > 0$ case, which is of interest in the context of periodic charge oscillations. The values of γ considered here are chosen so as to enable the evaluation of (D.1) by a straightforward extension of the procedure discussed in appendix B.1. As can be easily checked, this is achieved when $\gamma = 4, 6, 8, \cdots$.

By repeating the calculations from section B.1, integrating this time on the complex plane

$$\frac{\exp[ia \operatorname{sh}(z) \pm ib \operatorname{ch}(z)]}{\operatorname{sh}(z) \operatorname{ch}^{\gamma-1}(z)}, \tag{D.2}$$

we find that for $a \geq b > 0$ and the above-mentioned values of γ

$$I(a, b; \gamma) = \frac{\pi}{2} \cos(b) + \frac{\pi}{2} \text{Res} \left(\frac{\cos[b \, \text{ch}(z)] \exp[ia \, \text{sh}(z)]}{\text{sh}(z) \, \text{ch}^{\gamma-1}(z)}, \frac{i\pi}{2} \right). \tag{D.3}$$

It is then easy to argue that the residue from (D.3) can be written as $-P_\gamma(a, b) \exp(-a)$, where $P_\gamma(a, b)$ is a polynomial in a and b. For example,

$$P_4(a, b) = 1 + \frac{a}{2} - \frac{b^2}{2}, \tag{D.4}$$

$$P_6(a, b) = 1 + \frac{a^2}{8} - \frac{b^2}{2} + \frac{b^4}{24} + \frac{5a}{8} - \frac{ab^2}{4}, \tag{D.5}$$

$$P_8(a, b) = 1 + \frac{11a}{16} + \frac{3a^2}{16} + \frac{a^3}{48} - \frac{b^2}{2} - \frac{5ab^2}{16} - \frac{a^2b^2}{16} + \frac{b^4}{24} + \frac{ab^4}{48} - \frac{b^6}{720}. \tag{D.6}$$

We note that the highest power of a and b in $P_\gamma(a, b)$ is $\gamma/2 - 1$ and $\gamma - 2$, which can be easily proved.

Appendix E. Integral from expression (83): smoothness issues

We will discuss now the derivatives of

$$\widehat{I}(a, b; \gamma) = \int\limits_0^\infty d\omega \frac{\cos\left(b\sqrt{1 + \omega^2}\right)}{(1 + \omega^2)^{\gamma/2}} \frac{\sin(a\omega)}{a\omega}, \tag{E.1}$$

where

$$\gamma = 4, 6, 8, \cdots \tag{E.2}$$

so as to make the following discussion relevant to the considerations from section 6. We remark that under mapping (B.2)

$$\widehat{I}(a, b; \gamma) = I(a, b; \gamma)/a = \frac{2\pi^2}{qm} \phi(t, r; \gamma), \tag{E.3}$$

where $I(a, b; \gamma)$ and $\phi(t, r; \gamma)$ are given by (D.1) and (83), respectively.

To begin, we consider $\mathcal{I} : \Omega \times [0, \infty) \to \mathbb{R}$, where

$$\mathcal{I}(a, b, \omega; \gamma) = \frac{\cos\left(b\sqrt{1 + \omega^2}\right)}{(1 + \omega^2)^{\gamma/2}} \frac{\sin(a\omega)}{a\omega}, \tag{E.4}$$

$\Omega \ni (a, b)$ is an open set in $\mathbb{R}^2$

$$\Omega = (0, \infty) \times (0, \infty), \tag{E.5}$$

and

$$\frac{\sin(a\omega)}{a\omega} = 1 - \frac{(a\omega)^2}{3!} + \cdots \tag{E.6}$$

near and at $a\omega = 0$. These definitions lead to the following observations.

First, as far as the differentiability class of $\mathcal{I}$ is concerned, we observe that $\mathcal{I}(a, b, \omega; \gamma) \in C^{\gamma-2}(\Omega)$ for any $\omega \in [0, \infty)$.

Second, the map

$$\Omega \times [0, \infty) \ni (a, b, \omega) \mapsto \partial_a^\alpha \partial_b^\beta \mathcal{I}(a, b, \omega; \gamma) \in \mathbb{R} \tag{E.7}$$

is continuous for all

$$\alpha + \beta \le \gamma - 2, \tag{E.8a}$$

$$\alpha, \beta \in \mathbb{N}_0. \tag{E.8b}$$

Note that $\partial_x^\alpha = (\partial_x)^\alpha = \partial^\alpha / \partial x^\alpha$, where $x = a, b$.

Third, $\left| \partial_a^\alpha \partial_b^\beta \mathcal{I}(a, b, \omega; \gamma) \right|$ is upper bounded, for all (E.8) and $(a, b, \omega) \in \Omega \times [0, \infty)$, by the continuous function $u_{\alpha+\beta} : [0, \infty) \to \mathbb{R}$ such that $\int_0^\infty d\omega u_{\alpha+\beta}(\omega; \gamma) < \infty$. Namely,

$$u_{\alpha+\beta}(\omega; \gamma) = \begin{cases} 1 & \text{for} \quad 0 \le \omega \le 1 \\ \omega^{\alpha+\beta-\gamma} & \text{for} \quad \omega > 1 \end{cases}. \tag{E.9}$$

Such a result has been obtained with the help of the following inequality

$$\left| \frac{d^n}{dx^n} \frac{\sin(x)}{x} \right| \le \frac{1}{1+n} \le 1, \tag{E.10}$$

which is valid for $n \in \mathbb{N}_0$ and $x \in \mathbb{R}$ (see section 3.4.24 of [18] and references therein).

These three observations are sufficient for concluding that

$$\frac{\partial^\alpha}{\partial a^\alpha} \frac{\partial^\beta}{\partial b^\beta} \widehat{I}(a, b; \gamma) = \int_0^\infty d\omega \frac{\partial^\alpha}{\partial a^\alpha} \frac{\partial^\beta}{\partial b^\beta} \mathcal{I}(a, b, \omega; \gamma) \tag{E.11}$$

and $\widehat{I}(a, b; \gamma) \in C^{\gamma-2}(\Omega)$ [17]. Both conclusions are stated under the assumptions that (E.8) holds and $(a, b) \in \Omega$. In the following, we provide some comments related to (E.11).

E.1. Non-analyticity

We observe that (E.2) and (E.11) allow us to write

$$\partial_b^{\gamma-2} \widehat{I}(a, b; \gamma) = (-1)^{\gamma/2-1} I(a, b)/a \tag{E.12}$$

for $(a, b) \in \Omega$. Taking into account (B.26)–(B.28) and the non-existence of limits (C.17)–(C.19), it is easy to argue via (E.12) that $\widehat{I}(a, b; \gamma)$ is non-analytic. We mention in passing that the fact that the considered values of γ are even is crucial for the establishment of (E.12).

E.2. Klein-Gordon equation

We note that (E.11) can be used for showing that $I(a, b; \gamma)$ satisfies the $1 + 1$ dimensional Klein-Gordon equation

$$\frac{\partial^2}{\partial a^2} I(a, b; \gamma) - \frac{\partial^2}{\partial b^2} I(a, b; \gamma) = I(a, b; \gamma), \tag{E.13}$$

where a plays the role of the spatial coordinate, b plays the role of time, the mass is set to unity, $(a, b) \in \Omega$, and (E.2) is assumed. For $\gamma = 2$, $I(a, b; \gamma)$ turns into $I(a, b)$, which satisfies the Klein-Gordon equation for all $(a, b) \in \Omega$ except $a = b$ (this can be inferred from the discussion in appendix C). There is, however, the weaker form of the Klein-Gordon equation that holds without such a restriction when $\gamma = 2$ [see (C.20)].

References

[1] R. Greiner, J. Reinhardt, Field Quantization, Springer-Verlag, 1996.

[2] A.S. Goldhaber, M.M. Nieto, Photon and graviton mass limits, Rev. Mod. Phys. 82 (2010) 939.

[3] B.G.-g. Chen, D. Derbes, D. Griffiths, B. Hill, R. Sohn, Y.-S. Ting, Lectures of Sidney Coleman on Quantum Field Theory, World Scientific, 2018.

[4] S. Weinberg, The Quantum Theory of Fields, Vol. I: Foundations, Cambridge University Press, 2010.

[5] G.S. Guralnik, C.R. Hagen, T.W.B. Kibble, Global conservation laws and massless particles, Phys. Rev. Lett. 13 (1964) 585.

[6] G.S. Guralnik, C.R. Hagen, T.W.B. Kibble, Broken symmetries and the Goldstone theorem, in: R.L. Cool, R.E. Marshak (Eds.), Advances in Particle Physics, vol. 2, Interscience Publishers, 1968, pp. 567–708.

[7] J. Schwinger, Field theory commutators, Phys. Rev. Lett. 3 (1959) 296.

[8] E. Fabri, L.E. Picasso, Quantum field theory and approximate symmetries, Phys. Rev. Lett. 16 (1966) 408.

[9] M.P. Hertzberg, M. Jain, Ground state wave function overlap in superconductors and superfluids, Z. Naturforsch. A 75 (2020) 1063.

[10] M.P. Hertzberg, M. Jain, Counting of states in Higgs theories, Phys. Rev. D 99 (2019) 065015.

[11] I.S. Gradshteyn, I.M. Ryzhik, D. Zwillinger, V. Moll, Table of Integrals, Series, and Products, 8th ed., Academic Press, 2014.

[12] A. del Campo, G. García-Calderón, J. Muga, Quantum transients, Phys. Rep. 476 (2009) 1.

[13] N. Manton, P. Sutcliffe, Topological Solitons, Cambridge University Press, 2004.

[14] E.Y. Nugaev, A.V. Shkerin, Review of nontopological solitons in theories with $U(1)$-symmetry, J. Exp. Theor. Phys. 130 (2020) 301.

[15] L.-C. Tu, J. Luo, G.T. Gillies, The mass of the photon, Rep. Prog. Phys. 68 (2005) 77.

[16] S. Lang, Undergraduate Analysis, 2nd ed., Springer Science+Business Media, 1997.

[17] M. Jarnicki, Wykłady z analizy matematycznej I, II, III, IV, www2.im.uj.edu.pl/MarekJarnicki/lectures/analiza-1-2-3-4.pdf, 2015.

[18] D.S. Mitrinović, Analytic Inequalities, Springer-Verlag, 1970.